Extended Abstracts of the 2015 International Conference on Solid State Devices and Materials, Sapporo, 2015, pp24-25

Influence of *in-situ* Sb-Doping on Crystalline and Electrical Characteristics of *n*-type $Ge_{1-x}Sn_x$ Epitaxial Layer

J. Jeon[1], T. Asano[1, 2], W. Takeuchi[1], M. Kurosawa[1, 3], O. Nakatsuka[1], and S. Zaima[1, 3]
[1]Graduate School of Engineering, Nagoya University, Furo-cho, Chikusa-ku, Nagoya 464-8603, Japan
[2]Research Fellow of the Japan Society for the Promotion of Science, Japan
Phone: +81-52-789-3819, E-mail: jjeon@alice.xtal.nagoya-u.ac.jp
[3]EcoTopia Science Institute, Nagoya University, Furo-cho, Chikusa-ku, Nagoya 464-8603, Japan

Abstract

Aiming the formation of *n*-type $Ge_{1-x}Sn_x$, the *in-situ* Sb-doping on the $Ge_{1-x}Sn_x$ epitaxial growth with various Sb concentrations has been examined. The influences of Sb on crystalline and electrical characteristics of $Ge_{1-x}Sn_x$ epitaxial layer were investigated in detail. Effective *n*-type doping with Sb in $Ge_{1-x}Sn_x$ layer is confirmed by the Hall effect measurement. We also found that Sn-doping improves on the crystallinity and the surface morphology of $Ge_{1-x}Sn_x$ epitaxial layer.

1. Introduction

$Ge_{1-x}Sn_x$ is a promising group-IV semiconductor for next generation metal-oxide-semiconductor field effect transistors (MOSFET) because of the theoretically predicted higher mobilities of electron and hole than that of Ge [1]. In addition, $Ge_{1-x}Sn_x$ is familiar to the state-of-the-art Si process. Not only *p*-MOSFET but also *n*-MOSFET is required for low power consumption complementary MOS transistors, although *n*-type heavy doping technology for $Ge_{1-x}Sn_x$ is still on the process of developing [2] because the epitaxial growth of heavily doped n^+-$Ge_{1-x}Sn_x$ is difficult due to the low solubility of *n*-type dopants in Ge.

We focused *in-situ* Sb-doping in $Ge_{1-x}Sn_x$ to exceed the solid solubility and reduce the degradation of the growth layer. *In-situ* doping is a damage-free growth technique compared to ion implantation method. In addition, thanks to the low-temperature growth under the non-thermal equilibrium condition, we expect higher doping than the solubility limit of Sb and the suppression of the Sb segregation as well as Sn alloying. Also, the surfactant effect of Sb suppresses the three dimensional island growth, resulting in the two dimensional growth [3]. Thus, the control of Sb segregation and incorporation in $Ge_{1-x}Sn_x$ layer during the non-thermal equilibrium growth has a possibility realizing both a heavy doping and a high crystallinity. In this study, we examined *in-situ* Sb doping in $Ge_{1-x}Sn_x$ on Ge substrate for the formation of heavily doped *n*-type $Ge_{1-x}Sn_x$ epitaxial layer with a Sb concentration higher than 10^{20} cm^{-3}. We investigated the influence of Sb-doping on the crystallinity and electrical characteristics of $Ge_{1-x}Sn_x$ layers.

2. Sample preparation

P-type Ge(001) wafers were used as substrates. The substrates were chemically cleaned by dipping in aqueous ammonia and sulfuric acid solution. The substrates also was thermally cleaned at 430 °C for 30 min in an ultra-high vacuum molecular beam epitaxy (UHVMBE) chamber, with a base pressure less than 10^{-7} Pa. A Sb-doped $Ge_{1-x}Sn_x$ layer was grown on a substrate at 150 °C. Ge, Sn, and Sb were deposited with Knudsen cells (K-cells). The thicknesses of layers were ranged from 100 nm to 150 nm. The target Sn content in $Ge_{1-x}Sn_x$ was 6%. The Sb concentration was increased at the order of 10^{20} cm^{-3} by increasing K-cell temperatures of 220, 250, and 280 °C.

3. Results and discussion

Figures 1(a)-(c) show atomic force microscopy (AFM) images and surface profiles of $Ge_{1-x}Sn_x$ layers (a) without Sb and with Sb K-cell temperatures of (b) 220 and (c) 280°C. The $Ge_{1-x}Sn_x$ layer without Sb exhibits roughened surface indicating the Stranski-Krastanov growth mode. While the $Ge_{1-x}Sn_x$ layer with a low Sb concentration shows similar surface morphology to undoped one (**Fig. 1(b)**), increasing in the Sb concentration provides smooth and uniform surface of the $Ge_{1-x}Sn_x$ layer. **Figure 1(d)** shows the Sb K-cell temperature dependence of the root mean square (RMS) roughness of Sb-doped Ge and $Ge_{1-x}Sn_x$ layers. RMS of the Ge surface does not change regardless of the Sb concentration, while the RMS roughness of $Ge_{1-x}Sn_x$ surface decreases with increasing in the Sb concentration, because of the enhancement of two dimensional growth by the Sb doping. These results mean the surfactant effect of Sb appears with a sufficiently high Sb concentration.

Figure 2 shows the secondary ion mass spectroscopy (SIMS) depth profiles of Ge, Sn, and Sb for the $Ge_{1-x}Sn_x$:Sb(280 ºC)/Ge sample. Uniform depth profiles of both Sn and Sb are achieved with concentrations as high as 2×10^{20} and 2×10^{21} cm^{-3}, respectively. We considered that the low temperature MBE suppresses the Sb segregation and gives the high Sb concentration over the solubility limit in Ge. Also, it is confirmed that sufficiently heavy Sb doping brings the surfactant effect.

Figures 3 (a) and (b) show X-ray diffraction two dimensional reciprocal space mapping (XRD-2DRSM) results around the Ge$\bar{2}\bar{2}4$ Bragg reflection for $Ge_{1-x}Sn_x$/Ge samples without and with the Sb K-cell temperature of 280 ºC, respectively. The magnified logarithm peak profiles of the $Ge_{1-x}Sn_x$$\bar{2}\bar{2}4$ diffraction along the [110] direction are shown in **Fig. 3(c)**. The substitutional Sn content was estimated to be 5.5% through the diffraction peak position of $Ge_{1-x}Sn_x$ $\bar{2}\bar{2}4$ assuming the elastic deformation and Vegard's law. The reciprocal lattice, Q_y of the Sb-doped $Ge_{1-x}Sn_x$ layer shifts to a lower value as seen in **Figs. 3(a) and (b)**, although the Ge and Sn fluxes were same during the MBE growth. This means that Sb doping into substitutional site affects the strain in $Ge_{1-x}Sn_x$ epitaxial layer because the atomic radius of Sb is as well as Sn. The magnified peak profiles of $Ge_{1-x}Sn_x$$\bar{2}\bar{2}4$ along the [110] directions shows that the higher Sb K-cell temperature realizes a smaller broadening of the tail profile of the $Ge_{1-x}Sn_x$ diffraction peak, which means a high crystallinity.

This result indicates that Sb-doping enables to produce superior crystallinity of $Ge_{1-x}Sn_x$ epitaxial layers.

The sheet resistance, the carrier type, and the carrier concentration of $Ge_{1-x}Sn_x$ layers were measured by using micro four point probe (M4PP) and Hall effect measurements to estimate the electrically active Sb concentration as *n*-type dopant. **Figure 4** demonstrates the decrease in the sheet resistance of $Ge_{1-x}Sn_x$:Sb layer as a function of the Sb K-cell temperature. This indicates the increase in the electron concentration by Sb-doping. *N*-type conduction is observed with Hall effect measurements for Ge:Sb (280 ºC) and $Ge_{1-x}Sn_x$:Sb (280 ºC) with concentrations as high as 4.0×10^{20} cm^{-3} and 7.9×10^{20} cm^{-3} at the temperature of 197 K and 84 K, respectively.

4. Conclusions

In-situ Sb-doping realizes superior crystallinity and small surface roughness of $Ge_{1-x}Sn_x$ epitaxial layer. Low temperature growth with *in-situ* Sb-doping achieves heavily doped *n*-$Ge_{1-x}Sn_x$ epitaxial layers with an electron concentration of 7.9×10^{20} cm^{-3} and promises high performance of *n*-type $Ge_{1-x}Sn_x$ electronic applications.

Acknowledgements This work was partly supported by a Grant-in-Aid for Scientific Research (S) (No. 26220605) and (B) (No. 15H03565) from JSPS in Japan.

References

[1] J. D. Sau *et al.*, Phys. Rev. B **75**, 045208 (2007).
[2] K. Hozaki *et al.*, *in Abstract of IUMRS-ICEM2012*, Yokohama, Japan, Sept., 2012.
[3] H. J. Osten *et al.*, J. Vac. Sci. Technol. B **10**, 1151 (1992).

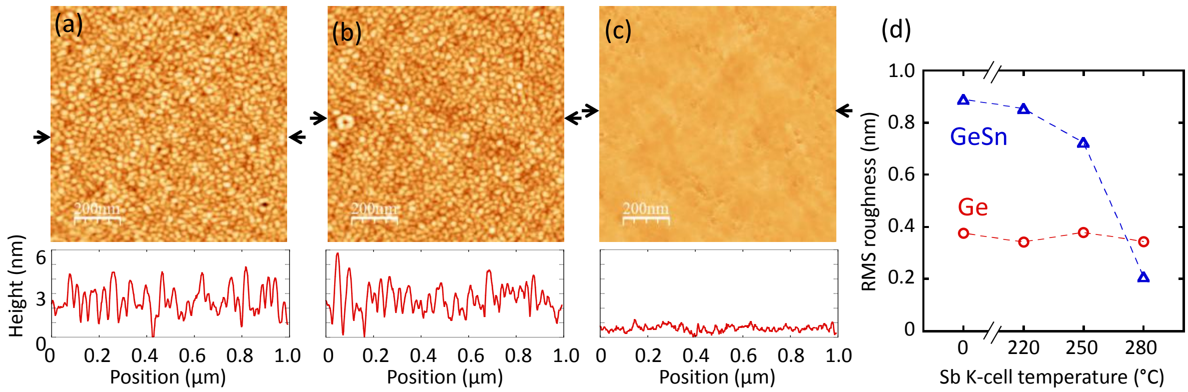

Fig. 1. AFM images and line profiles of $Ge_{1-x}Sn_x$ layers (a) without and with Sb-doping grown with Sb K-cell temperatures of (a) 0 °C, (b) 220, and (c) 280°C. (d) Sb concentration dependence of RMS roughness of Ge:Sb and $Ge_{1-x}Sn_x$:Sb layers.

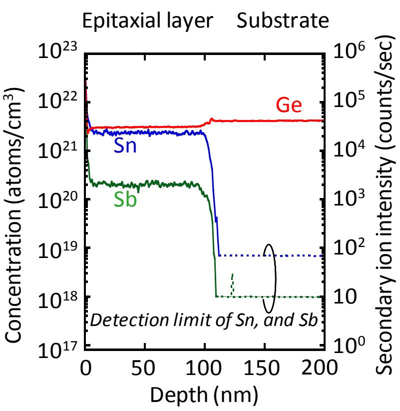

Fig. 2. SIMS depth profiles of Ge, Sn, and Sb for the $Ge_{1-x}Sn_x$:Sb(280°C) sample.

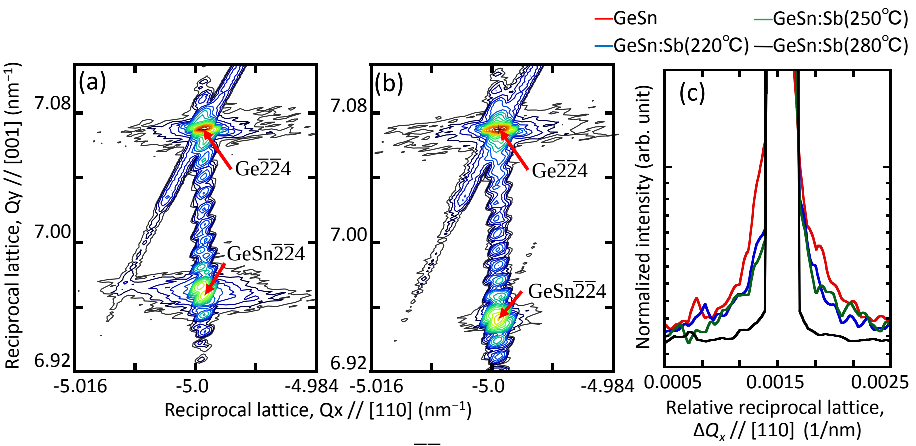

Fig. 3. XRD-2DRSM results around Ge$\bar{2}\bar{2}4$ Bragg reflection of $Ge_{1-x}Sn_x$ layers (a) without and (b) with Sb doping grown on Ge substrates. Sb K-cell temperature was 280ºC. (c) The magnified logarithm peak profiles of $Ge_{1-x}Sn_x\bar{2}\bar{2}4$ along the [110] directions.

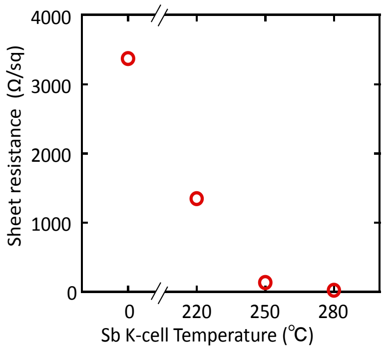

Fig. 4. The Sb k-cell temperature dependence of the sheet resistance for $Ge_{1-x}Sn_x$:Sb samples by using M4PP method.